



Cite this: *Chem. Commun.*, 2014, 50, 10979

Received 14th July 2014,
Accepted 28th July 2014

DOI: 10.1039/c4cc05421k

www.rsc.org/chemcomm

Stepwise assembly of an adamantoid Ru_4Ag_6 cage by control of metal coordination geometry at specific sites†

Alexander J. Methereil and Michael D. Ward*

The geometrically pure 'complex ligand' $\text{fac}[\text{Ru}(\text{L}^{\text{Ph}})_3]^{2+}$, in which three pendant bidentate binding sites are located on one face of the complex, reacts with $\text{Ag}(\text{I})$ ions to form the adamantoid decanuclear cage $[\{\text{Ru}(\text{L}^{\text{Ph}})_3\}_4\text{Ag}_6](\text{PF}_6)_{14}$ which contains a 6-coordinate $\text{Ru}(\text{II})$ ion at each vertex of a large tetrahedron and a 4-coordinate $\text{Ag}(\text{I})$ ion along each edge.

The self-assembly and host-guest chemistry of metal-ligand coordination cages continue to fascinate. Such high-symmetry cages represent appealing synthetic targets for supramolecular chemists to test their skills at controlling self-assembly so as to generate elaborate, multi-component assemblies from simple starting materials.¹ In addition the ability of cages to bind guest molecules in their central cavity leads to potential applications² ranging from catalysis³ to drug delivery.⁴

The vast majority of cages are formed from just two types of component: one type of metal ion and one type of ligand. A few examples of mixed-ligand cages are known in which the self-assembly process specifically occurs with selection of two different types of ligand, resulting in a heteroleptic complex being favoured over the homoleptic alternatives.⁵ Likewise a few examples of mixed-metal cages exist in which two different types of metal ion occupy different vertex positions in a cage structure.^{6–8} This can occur when the two types of metal ion have different geometric preferences and the self-assembly requires both: for example, octahedral tris-chelate metal ions at the vertices of a cube and square planar ions with four monodentate ligands at the face centres.⁷ Alternatively, we showed recently how different types of metal ion can be positioned at specific sites in a polyhedral array if kinetically inert metal complex subcomponents

are prepared first and then combined with a second labile metal ion to complete the assembly in a stepwise manner.⁸

Our extensive family of polyhedral cage complexes generally contain an octahedral tris-chelate metal ion at each vertex, and a bis-bidentate bridging ligand (containing two pyrazolyl-pyridine chelating termini) along each edge.^{1c} In these complexes the geometric isomerism (*fac* vs. *mer*) of the metal centres turns out to play a crucial role in the nature of the assembly that forms. In some complexes, such as a family of M_4L_6 tetrahedra, all four metal centres have a *fac* tris-chelate geometry;⁹ in contrast, in a series of $\text{M}_{12}\text{L}_{18}$ truncated tetrahedra, all metal centres have a *mer* tris-chelate geometry.¹⁰ In several other types of cage assembly however there is a 3 : 1 mixture of *mer* : *fac* tris-chelate vertices.¹¹ Therefore, the ability to control the self-assembly of such cages – particularly mixed-metal versions – relies on the ability to prepare kinetically stable, geometrically pure *fac* or *mer* tris-chelate sub-components as starting points to propagate a specific assembly.

We report here the use of this principle – *viz.* control of geometric isomerism at specific sites in a cage as a way of directing assembly – in the formation of an unusual $[\text{Ru}_4\text{Ag}_6(\text{L}^{\text{Ph}})_{12}]^{14+}$ mixed-metal cage which combines octahedral *fac* tris-chelate $\text{Ru}(\text{II})$ vertices and pseudo-tetrahedral $\text{Ag}(\text{I})$ bis-chelate edges in an adamantane-type cage structure having tetrahedral symmetry. The novelty lies both in the structure of the cage [a combination of three-connected and two-connected metal vertices based on $\text{Ru}(\text{II})$ and $\text{Ag}(\text{I})$ respectively], and in the use of the pre-formed, kinetically stable $[\text{Ru}(\text{L}^{\text{Ph}})_3]^{2+}$ units as purely the *fac* isomer to direct the course of the self-assembly.

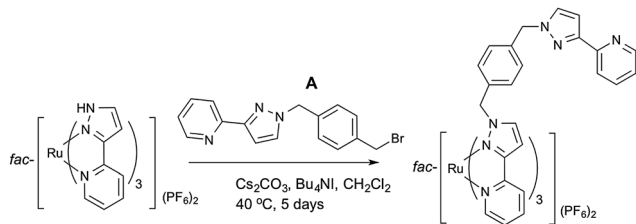
As *fac*- $[\text{ML}_3]^{2+}$ units from this family occur at specific sites in many of our cages,^{1c} we wished to start with *fac*- $[\text{Ru}(\text{L}^{\text{Ph}})_3]^{2+}$ in which the three pendant binding sites, where cage propagation occurs by coordination to additional metal ions, have a *fac* arrangement. Simple reaction of $\text{Ru}(\text{dmsO})_4\text{Cl}_2$ with > 3 equivalents of L^{Ph} afforded $[\text{Ru}(\text{L}^{\text{Ph}})_3]^{2+}$ as a 1 : 3 statistical mixture of *fac* : *mer* isomers as shown by the ^1H NMR spectrum in which every type of proton (*e.g.* coordinated pyridyl H^6) occurred in four different environments in a 1 : 1 : 1 : 1 ratio. However column chromatography or HPLC under a range of conditions did not give a good separation of the geometric isomers.

Department of Chemistry, University of Sheffield, Sheffield S3 7HF, UK.

E-mail: m.d.ward@sheffield.ac.uk

† Electronic supplementary information (ESI) available: Crystallographic data in CIF format; details of crystallographic data collections and refinements; selected bond distances for the structures; synthesis and characterisation of new complexes, including ^1H NMR, COSY and DOSY spectra; additional figures of the cage $[\{\text{Ru}(\text{L}^{\text{Ph}})_3\}_4\text{Ag}_6](\text{PF}_6)_{14}$. CCDC 1013864 and 1013865. For ESI and crystallographic data in CIF or other electronic format see DOI: 10.1039/c4cc05421k



Scheme 1 Preparation of fac -[Ru(L^{Ph})₃](PF₆)₂.

We therefore went back a step in the synthesis, to fac -[Ru(PyPzH)₃]²⁺ [Scheme 1; PyPzH = 3-(2-pyridyl)-pyrazole] which can be readily separated from the *mer* isomer using a method reported earlier.¹² In fac -[Ru(PyPzH)₃]²⁺ the three pyrazole rings, with their acidic NH protons, lie of course on the same face of the complex. Alkylation of these^{12a} with the bromomethyl compound **A** completed the formation of the L^{Ph} ligands coordinated to the metal centre at one end, to give fac -[Ru(L^{Ph})₃]²⁺ which was isolated as the hexafluorophosphate salt (see ESI[†]). The ¹H NMR spectrum showed 20 ¹H environments confirming the threefold symmetry with all three ligands equivalent. Notably the CH₂ protons close to the Ru(II) chiral centre are diastereotopic, giving a coupled pair of doublets at 5.5 and 4.8 ppm, whereas the CH₂ protons more remote from the Ru(II) centre give a singlet at 5.3 ppm (Fig. S3, ESI[†]). The crystal structure of the complex cation of fac -[Ru(L^{Ph})₃](PF₆)₂·acetone is shown in Fig. 1; (ESI[†]) it is clear how the three pendant pyrazolyl-pyridine arms are directed to the same face of the complex. The phenyl group of each pendant arm forms a π -stacking interaction with a coordinated pyrazolyl-pyridine group from another ligand, as we have observed in related complexes.

Ag(I) generally forms four-coordinate bis-chelate complexes with pyrazolyl-pyridine ligands of this type.¹³ On the basis that three pendant bidentate sites are available for coordination in fac -[Ru(L^{Ph})₃](PF₆)₂, we combined (ESI[†]) fac -[Ru(L^{Ph})₃](PF₆)₂ with 1.5 equivalents of AgPF₆ to maximise the likelihood of a structure forming that conforms to the principle of maximum site occupancy, with all metal ions coordinatively saturated and

all ligands fully coordinated.¹⁴ If each pendant ligand fragment coordinates to a different Ag(I) ion, as is likely on steric grounds given the distance between the pendant pyrazolyl-pyridine units, we expect a mixed-metal cage in which each fac -[Ru(L^{Ph})₃]²⁺ unit caps a triangular array of Ag(I) ions.

Slow crystallisation of the reaction mixture afforded X-ray quality crystals of what proved to be a decanuclear Ru₄Ag₆ cage [Ru(L^{Ph})₃]₄Ag₆(PF₆)₁₄ (Fig. 2–4) (ESI[†]). The cage has an adamantane-like structure, with a Ru(II) tris-chelate unit at each of the four three-connected vertices which are arranged in an approximate tetrahedron. An Ag(I) bis-chelate unit occupies each of the six two-connected vertices. Thus the structure can be described as a tetrahedral array of Ru(II) ions with an Ag(I) ion lying in the centre of each Ru···Ru edge (Fig. 2), with every adjacent Ru(II)–Ag(I) pair connected by a bis-bidentate bridging ligand L^{Ph}.

The molecule lies astride a crystallographic C₂ axis such that half of it is unique. This axis passes through Ag(2) and Ag(3) such that these lie on special positions with 50% occupancy in the asymmetric unit, whereas Ag(1) and Ag(4) are in general positions. There is a (non-crystallographic) C₃ axis through each Ru(II) tris-chelate vertex, with all four being homochiral; thus the complex belongs to the pure rotation symmetry point group *T* which is a common consequence of removing mirror planes from high-symmetry polyhedra.

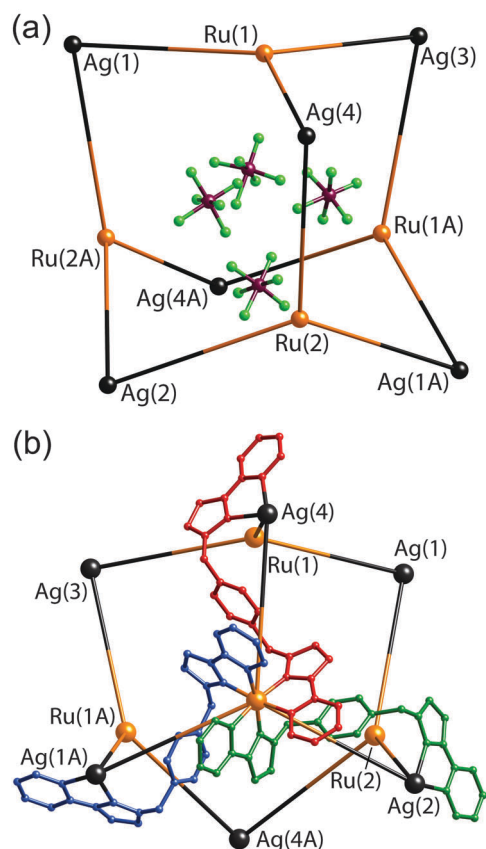


Fig. 2 Two views of the structure of [Ru(L^{Ph})₃]₄Ag₆(PF₆)₁₄: (a) the adamantane-like arrangement of metal ions, with the four anions that lie within the cavity also shown; (b) the metal superstructure with three of the bridging ligands included (coloured differently for clarity).

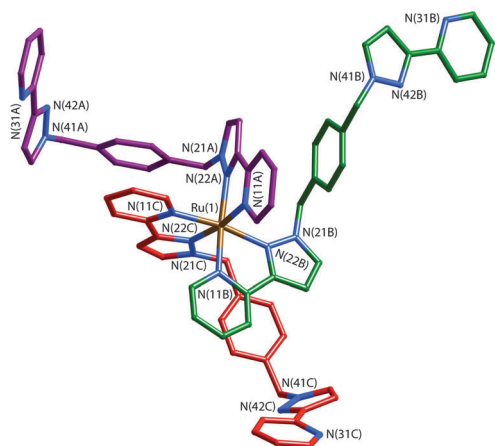


Fig. 1 Structure of the complex cation of fac -[Ru(L^{Ph})₃](PF₆)₂·acetone with the three ligands coloured differently for clarity.



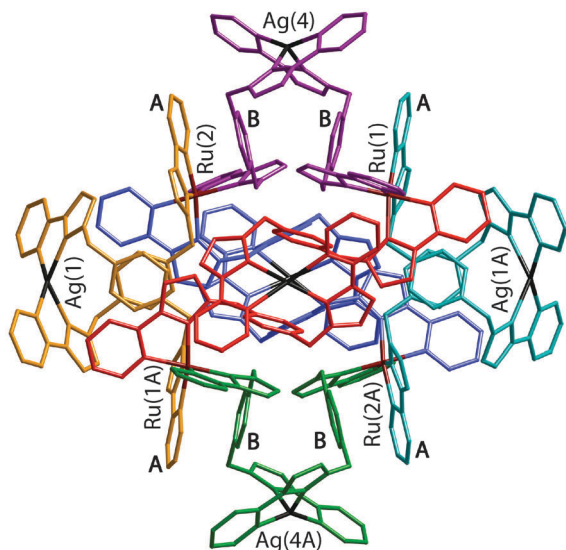


Fig. 3 A view of the complete complex cation of $[(\text{Ru}(\text{L}^{\text{Ph}})_3)_4\text{Ag}_6](\text{PF}_6)_{14}$. The two ligands coordinated to each $\text{Ag}(\text{I})$ have the same colour. Labels A and B denote the electron-deficient (pyrazolyl-pyridine) and electron-rich (phenyl) units involved in the pairwise π -stacking interactions.

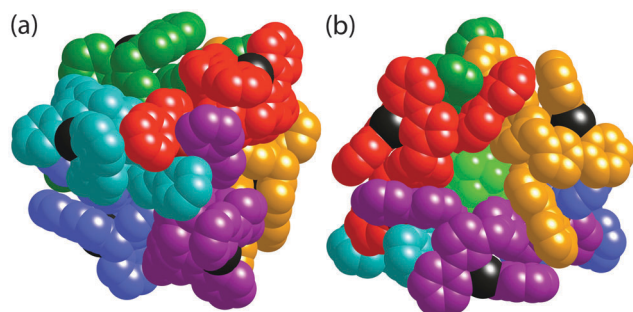


Fig. 4 Space-filling views of the complex cation of $[(\text{Ru}(\text{L}^{\text{Ph}})_3)_4\text{Ag}_6](\text{PF}_6)_{14}$. (a) A view down one of the threefold axes, through a $\text{Ru}(\text{II})$ tris-chelate centre; (b) a view from the opposite side of the complex looking at one of the Ru_3Ag_3 faces, with one of the encapsulated $[\text{PF}_6]^-$ anions (F atoms in green) visible through the portal.

The six $\text{Ag}(\text{I})$ ions lie on the three C_2 axes associated with T symmetry of which one [the $\text{Ag}(\text{2}) \cdots \text{Ag}(\text{3})$ axis, as mentioned above] occurs in the crystal structure; necessarily, all six $\text{Ag}(\text{I})$ ions have the same chirality associated with their two non-symmetrical chelating ligands. The nearest-neighbour $\text{Ru} \cdots \text{Ag}$ separations (*i.e.* along an edge spanned by a bridging ligand) lie in the range 8.86–9.32 Å, averaging 9.06 Å.

The flexibility of the ligands associated with the CH_2 ‘hinges’ allows them to adopt a conformation which maximises inter-ligand π -stacking – a key driver for assembly of such cages.^{16,15} This can be seen in the view shown in Fig. 3, in which the octahedral disposition of the six $\text{Ag}(\text{I})$ ions is emphasised with these being placed top/bottom, left/right and front/back with each pair of $\text{Ag}(\text{I})$ ions lying on a C_2 axis. In this view, $\text{Ag}(\text{4})/\text{Ag}(\text{4A})$ form the ‘vertical’ C_2 axis. The two ligands attached to each $\text{Ag}(\text{I})$ ion have the same colour (*i.e.* the twelve ligands are coloured in six sets of two). The ligands

are disposed such that a central phenyl ring of a bridging ligand (denoted ‘B’ in Fig. 3) lies parallel to, and overlapping with, a pyrazolyl-pyridine unit of another ligand coordinated to the adjacent $\text{Ru}(\text{II})$ ion (denoted ‘A’ in Fig. 3), forming a charge-assisted π -stack between electron-rich (phenyl) and electron-deficient (coordinated pyrazolyl-pyridine) ligands. In the view in Fig. 3 we can readily see four such A/B stacked pairs; there are necessarily, therefore, twelve such interactions overall – involving every phenyl group – as the orientations with $\text{Ag}(\text{1})/\text{Ag}(\text{1A})$ and $\text{Ag}(\text{2})/\text{Ag}(\text{2A})$ as the ‘vertical’ axis are equivalent.

An alternative space-filling view, looking down one of the C_3 axes associated with a $\text{Ru}(\text{II})$ tris-chelate centre, is in Fig. 4a. The cage complex has an approximate cavity size of 178 Å³ (calculated assuming that the windows are blocked; Fig. S2, ESI†). The cavity is occupied by a tetrahedral array of four $[\text{PF}_6]^-$ anions (Fig. 2a), each one blocking the window in one of the Ru_3Ag_3 faces of the cage, as shown in Fig. 4b in which three of the F atoms of the $[\text{PF}_6]^-$ anion in that window can be clearly seen. The P \cdots P separations between the four encapsulated anions are in the range of 5.44–5.61 Å, resulting in peripheral F \cdots F contacts between anions of ≈ 3 Å, which is the sum of the van der Waals’ radii of two F atoms. Each anion is involved in a range of $\text{CH} \cdots \text{F}$ interactions with ligand H atoms. Fig. S1(a) (ESI†) shows one of the anions embedded in the window in one of the Ru_3Ag_3 faces, with dotted lines indicating some of the short non-bonded $\text{C} \cdots \text{F}$ contacts (≤ 3.15 Å) which are indicative of weak hydrogen-bonding interactions between anion and ligand. This view also nicely shows how the array of six ligands around each Ru_3Ag_3 face forms a cyclic helicate with every ligand in the cycle having the same sense of ‘under and over’ around the ring. Fig. S1(b) (ESI†) shows how the four anions fill the cavity.

The structural integrity of the complex in solution was confirmed by ES mass spectrometry, which showed peaks corresponding to the species $[(\text{Ru}_4\text{Ag}_6(\text{L}^{\text{Ph}})_{12})(\text{PF}_6)_{14-n}]^{n+}$ ($n = 3, 4, 6$), and also by ^1H NMR spectroscopy (ESI†). The ^1H NMR spectrum at room temperature is very broad, indicative of molecular motions [possibly associated with the highly flexible $\text{Ag}(\text{I})$ centres] at a rate comparable to the ^1H NMR timescale. However at 75 °C the spectrum sharpened satisfactorily and showed the expected 20 independent ^1H signals associated with one environment for L^{Ph} with no internal symmetry (Fig. S6, ESI†); this spectrum is considerably different from that of *fac*- $[\text{Ru}(\text{L}^{\text{Ph}})_3](\text{PF}_6)_2$. Significantly, the chirality associated with the $\{\text{Ag}(\text{NN})_2\}^+$ centres ensures that *both* independent sets of CH_2 protons are now diastereotopic, giving two pairs of coupled doublets in the 4.5–5.5 ppm region (Fig. S5, ESI†). That this species is a large assembly is confirmed by its DOSY spectrum which clearly shows that all of its ^1H signals belong to a single species which has a much lower diffusion rate [$\log D$ ($\text{m}^2 \text{s}^{-1}$) = -9.2] than *fac*- $[\text{Ru}(\text{L}^{\text{Ph}})_3](\text{PF}_6)_2$ [$\log D$ ($\text{m}^2 \text{s}^{-1}$) = -8.4] (Fig. S7, ESI†).

Assembly of this cage with its adamantane-like structure thus relies on two different types of geometric control at specific metal sites. Firstly it requires the appropriate combination of metal vertices that are three-connected [each tris-chelate, $\text{Ru}(\text{II})$ ion is connected to three $\text{Ag}(\text{I})$ ions] and two connected [each bis-chelate $\text{Ag}(\text{I})$ ion is connected to two $\text{Ru}(\text{II})$ ions]. This is achieved by using metal ions with different stereoelectronic preference, *i.e.* a combination of



6-coordinate Ru(II) and 4-coordinate Ag(I) ions at alternating sites. Secondly, the structure relies on exclusive use of pre-formed, kinetically inert *fac* isomers of the $[\text{Ru}(\text{L}^{\text{ph}})_3]^{2+}$ unit. We note that there are a few other examples of mixed-metal $\text{M}_6\text{M}'_4(\mu\text{-L})_{10}$ complexes with an adamantane-like core structure.^{16,17} Many of these arise from one-pot reactions, but some – which use cyanide bridges along the M–M' edges – are based on a kinetically stable, pre-formed hexacyanometallate unit as one precursor in a manner related to ours.¹⁷ In principle the method we have reported here should have high generality as it could be extended to other kinetically inert octahedral d^6 metal complexes of the type *fac*- $[\text{M}(\text{PyPzH})_3]^{n+}$ (M = Os, $n = 2$; M = Rh, Ir, $n = 3$ etc.).

We thank EPSRC for financial support, Mr Will Cullen for assistance with the NMR measurements, and the EPSRC National Crystallography Service for the crystallographic data collections.

Notes and references

- (a) D. Fiedler, D. H. Leung, R. G. Bergman and K. N. Raymond, *Acc. Chem. Res.*, 2005, **38**, 349; (b) M. Fujita, M. Tominaga, A. Hori and B. Therrien, *Acc. Chem. Res.*, 2005, **38**, 369; (c) M. D. Ward, *Chem. Commun.*, 2009, 4487; (d) J. J. Perry, J. A. Perman and M. J. Zaworotko, *Chem. Soc. Rev.*, 2009, **38**, 1400; (e) H. Amouri, C. Desmarests and J. Moussa, *Chem. Rev.*, 2012, **112**, 2015; (f) A. F. Williams, *Coord. Chem. Rev.*, 2011, **255**, 2104; (g) Z. Laughrey and B. Gibb, *Chem. Soc. Rev.*, 2011, **40**, 363; (h) P. Jin, S. J. Dalgarno and J. L. Atwood, *Coord. Chem. Rev.*, 2012, **254**, 1760; (i) R. J. Chakrabarty, P. S. Mukherjee and P. J. Stang, *Chem. Rev.*, 2011, **111**, 6810; (j) Y. Inokuma, M. Kawano and M. Fujita, *Nat. Chem.*, 2011, **3**, 349; (k) M. D. Pluth, R. G. Bergman and K. N. Raymond, *Acc. Chem. Res.*, 2009, **42**, 1650; (l) M. M. J. Smulders, I. A. Riddell, C. Browne and J. R. Nitschke, *Chem. Soc. Rev.*, 2013, **42**, 1728; (m) T. Nakamura, H. Ube and M. Shionoya, *Chem. Lett.*, 2014, **42**, 328.
- M. D. Ward and P. R. Raithby, *Chem. Soc. Rev.*, 2013, **42**, 1619.
- (a) C. J. Brown, R. G. Bergman and K. N. Raymond, *J. Am. Chem. Soc.*, 2009, **131**, 17530; (b) C. J. Hastings, M. D. Pluth, R. G. Bergman and K. N. Raymond, *J. Am. Chem. Soc.*, 2010, **132**, 6938; (c) J. L. Bolliger, A. M. Belenguer and J. R. Nitschke, *Angew. Chem., Int. Ed.*, 2013, **52**, 7958.
- (a) J. W. Yi, N. P. E. Barry, M. A. Furrer, O. Zava, P. J. Dyson, B. Therrien and B. H. Kim, *Bioconjugate Chem.*, 2012, **23**, 461; (b) B. Therrien, *Chem. – Eur. J.*, 2013, **19**, 8378; (c) J. E. M. Lewis, E. L. Gavey, S. A. Cameron and J. D. Crowley, *Chem. Sci.*, 2012, **3**, 778.
- (a) N. K. Al-Rasbi, I. Tidmarsh, S. P. Argent, H. Adams, L. P. Harding and M. D. Ward, *J. Am. Chem. Soc.*, 2008, **130**, 11641; (b) S. Hiraoka, Y. Kubota and M. Fujita, *Chem. Commun.*, 2000, 1509; (c) S. Hiraoka, M. Shiro and M. Shionoya, *J. Am. Chem. Soc.*, 2004, **126**, 1214; (d) P. N. W. Baxter, J.-M. Lehn, G. Baum and D. Fenske, *Chem. – Eur. J.*, 1999, **5**, 102; (e) B. Olenyuk, J. A. Whiteford, A. Fechtenkötter and P. J. Stang, *Nature*, 1999, **398**, 796; (f) M. Wang, Y.-R. Zheng, K. Ghosh and P. J. Stang, *J. Am. Chem. Soc.*, 2010, **132**, 6282; (g) J.-R. Li and H.-C. Zhou, *Angew. Chem., Int. Ed.*, 2009, **48**, 8465.
- (a) W. J. Ramsay, T. K. Ronson, J. K. Clegg and J. R. Nitschke, *Angew. Chem., Int. Ed.*, 2013, **52**, 13439; (b) X. Sun, D. W. Johnson, D. L. Caulder, K. N. Raymond and E. H. Wong, *J. Am. Chem. Soc.*, 2001, **123**, 2752; (c) F. E. Hahn, M. Offermann, C. Schulzelsfort, T. Pape and R. Frohlich, *Angew. Chem., Int. Ed.*, 2008, **47**, 6794; (d) S. Hiraoka, Y. Sakata and M. Shionoya, *J. Am. Chem. Soc.*, 2008, **130**, 10058; (e) H.-B. Wu and Q.-M. Wang, *Angew. Chem., Int. Ed.*, 2009, **48**, 7343; (f) A. J. Metherell and M. D. Ward, *RSC Adv.*, 2013, **3**, 14281.
- (a) M. L. Saha and M. Schmittle, *J. Am. Chem. Soc.*, 2013, **135**, 17743; (b) M. M. J. Smulders, A. Jimenez and J. R. Nitschke, *Angew. Chem., Int. Ed.*, 2012, **51**, 6681; (c) K. Li, L.-Y. Zhang, C. Yan, M. Pan, L. Zhang and C.-Y. Su, *J. Am. Chem. Soc.*, 2014, **136**, 4456; (d) F. Reichel, J. K. Clegg, K. Gloe, K. Gloe, J. J. Weigand, J. K. Reynolds, C.-G. Li, J. R. Aldrich-Wright, C. J. Kepert, L. F. Lindoy, H.-C. Yao and F. Li, *Inorg. Chem.*, 2014, **53**, 688; (e) M. Otte, P. F. Kuijpers, O. Troeppner, I. Ivanović-Burmazović, J. N. H. Reek and B. de Bruin, *Chem. – Eur. J.*, 2013, **19**, 10170; (f) A. Galstyan, P. J. Sanz Miguel, K. Weise and B. Lippert, *Dalton Trans.*, 2013, **42**, 16151; (g) P. de Wolf, S. L. Heath and J. A. Thomas, *Chem. Commun.*, 2002, 2540.
- A. J. Metherell and M. D. Ward, *Chem. Commun.*, 2014, **50**, 6330.
- (a) J. S. Fleming, K. L. V. Mann, C.-A. Carraz, E. Psillakis, J. C. Jeffery, J. A. McCleverty and M. D. Ward, *Angew. Chem., Int. Ed.*, 1998, **37**, 1279; (b) R. L. Paul, Z. R. Bell, J. C. Jeffery, J. A. McCleverty and M. D. Ward, *Proc. Natl. Acad. Sci. U. S. A.*, 2002, **99**, 4883; (c) I. S. Tidmarsh, B. F. Taylor, M. J. Hardie, L. Russo, W. Clegg and M. D. Ward, *New J. Chem.*, 2009, **33**, 366.
- (a) Z. R. Bell, J. C. Jeffery, J. A. McCleverty and M. D. Ward, *Angew. Chem., Int. Ed.*, 2002, **41**, 2515; (b) S. P. Argent, H. Adams, T. Riis-Johannessen, J. C. Jeffery, L. P. Harding, O. Mamula and M. D. Ward, *Inorg. Chem.*, 2006, **45**, 3905.
- (a) I. S. Tidmarsh, T. B. Faust, H. Adams, L. P. Harding, L. Russo, W. Clegg and M. D. Ward, *J. Am. Chem. Soc.*, 2008, **130**, 15167; (b) A. Stephenson, S. P. Argent, T. Riis-Johannessen, I. S. Tidmarsh and M. D. Ward, *J. Am. Chem. Soc.*, 2011, **133**, 858; (c) B. R. Hall, L. E. Manck, I. S. Tidmarsh, A. Stephenson, B. F. Taylor, E. J. Blaikie, D. A. Vander Griend and M. D. Ward, *Dalton Trans.*, 2011, **40**, 12132.
- (a) A. J. Metherell, W. Cullen, A. Stephenson, C. A. Hunter and M. D. Ward, *Dalton Trans.*, 2014, **43**, 71; (b) M. H. W. Lam, S. T. C. Cheung, K.-M. Fung and W.-T. Wong, *Inorg. Chem.*, 1997, **36**, 4618.
- (a) A. Stephenson and M. D. Ward, *Chem. Commun.*, 2012, **48**, 3605; (b) A. Stephenson and M. D. Ward, *RSC Adv.*, 2012, **2**, 10844.
- J.-M. Lehn and A. V. Eliseev, *Science*, 2001, **291**, 2331.
- A. Stephenson, D. Sykes and M. D. Ward, *Dalton Trans.*, 2013, **42**, 6756.
- (a) L. Wang, Y. Li, Y. Peng, Z. Liang, J. Yu and R. Xu, *Dalton Trans.*, 2012, **41**, 6242; (b) X. Kuang, X. Wu, R. Yu, J. P. Donahue, J. Huang and C.-Z. Lu, *Nat. Chem.*, 2010, **2**, 461.
- (a) T. Shiga, F. Iijima, T. Tetsuka, G. N. Newton and H. Oshio, *Macromol. Symp.*, 2012, **317–318**, 286; (b) T. Shiga, G. N. Newton, J. S. Mathieson, T. Tetsuka, M. Nihei, L. Cronin and H. Oshio, *Dalton Trans.*, 2010, **39**, 4730; (c) T. Shiga, T. Tetsuka, K. Sakai, Y. Sekine, M. Nihei, G. N. Newton and H. Oshio, *Inorg. Chem.*, 2014, **53**, 5899.

